Title

Repeatability of Contour Method Residual Stress Measurements for a Range of Materials, Processes, and Geometries

Journal

Materials Performance and Characterization, 7(4)

ISSN

2379-1365

Authors

Olson, Mitchell D
DeWald, Adrian T
Hill, Michael R

Publication Date

2018-11-07

DOI

10.1520/mpc20170044

Repeatability of contour method residual stress measurements for a range of material, process, and geometry

Mitchell D. Olson[1], Adrian T. DeWald[1], and Michael R. Hill[2*]

[1]*Hill Engineering, LLC, 3083 Gold Canal Drive, Rancho Cordova, CA, USA*
[2]*University of California, Davis, Department of Mechanical and Aerospace Engineering, One Shields Avenue, Davis, CA, USA*

Submitted for the Special Issue on Residual Stress in the
ASTM International Journal on Materials Performance and Characterization, April 2017
Submitted in revised form, August 2017; Accepted, September 2017

Final Citation: Olson, M., DeWald, A., and Hill, M. "Repeatability of Contour Method Residual Stress Measurements for a Range of Materials, Processes, and Geometries," Materials Performance and Characterization, Vol. 7, No. 4, 2018, https://doi.org/10.1520/MPC20170044. ISSN 2379-1365

Abstract

This paper examines precision of the contour method using five residual stress measurement repeatability studies. The test specimens evaluated include: an aluminum T-section, a stainless steel plate with a dissimilar metal slot-filled weld, a stainless steel forging, a titanium plate with an electron beam slot-filled weld, and a nickel disk forging. These specimens were selected to encompass a range of typical materials and residual stress distributions. Each repeatability study included contour method measurements on 5 to 10 similar specimens. Following completion of the residual stress measurements an analysis was performed to determine the repeatability standard deviation of each population. In general, the results of the various repeatability studies are similar. The repeatability standard deviation tends to be relatively small throughout the part interior and there are localized regions of higher repeatability standard deviation along the part perimeter. The repeatability standard deviations over most of the cross-section range from 5 MPa, for the aluminum T-section, to 25 MPa for the nickel disk forging. There is a strong correlation between the elastic modulus of the material and the repeatability standard deviation. These results provide demonstrated precision of the contour method over a broad range of specimen geometry, material, and stress state.

Keywords: Repeatability, repeatability standard deviation, measurement repeatability, precision, contour method, residual stress

1. Introduction

Precision is an important parameter to consider when selecting a measurement technique since it provides the expected measurement variability for a given test method. The definition of precision is the closeness of agreement between independent test results obtained under stipulated conditions. Precision

* Corresponding author. *E-mail address:* mrhill@ucdavis.edu

is closely related to measurement repeatability. Repeatability is the precision where the stipulated conditions require that the same test method is applied to identical test specimens, in the same laboratory, by the same operator, over a short interval of time [1]. Repeatability is quantified by the repeatability standard deviation, which is simply the standard deviation of test results from a repeatability study.

It is noted that the determination of the precision of a measurement does not quantify the measurement accuracy, which is determined by comparing the closeness of a test result to an accepted reference standard [1]. There are no perfect reference standards available for residual stress measurements, which limits quantification of residual stress measurement accuracy. Inter-method comparisons are often used to provide insight into measurement accuracy [2,3,4,5] as well as experiments on specimens having an expected residual stress field found from an analytical model [6,7]. This paper is intended to address measurement repeatability, not measurement accuracy.

The repeatability of the contour method has been determined in prior publications in a quenched aluminum bar [8] and a stainless steel plate with a stainless steel slot-filled weld [9]. The repeatability study in the quenched aluminum bar found a stress field that had large magnitude compressive stress along the bar periphery (around -175 MPa) and tensile stress at the center of the bar (around 175 MPa). The repeatability standard deviation was between 5 and 10 MPa over most of the cross-section, with localized regions at the periphery having larger repeatability standard deviation (maximum as large as 20 MPa). The repeatability study in the stainless steel plate found repeatability standard deviation under 20 MPa at most locations, with localized regions up to 30 MPa.

The primary objective of the present study is to build on the prior studies [8,9] and determine contour method repeatability under a representative set of conditions. The set of conditions includes

alloys of iron, aluminum, titanium, and nickel, reflecting key industrial alloys. The set of conditions also includes a range of geometry, including plate, disk, and structural section.

2. Methods

2.1. OVERVIEW

Contour method repeatability was assessed in five different configurations: an aluminum T-section, a stainless steel plate with a dissimilar metal (DM) slot-filled weld, a stainless steel forging, a titanium plate with an electron beam (EB) slot-filled weld, and a nickel alloy disk. Each repeatability assessment included contour method measurements on sets of replicate specimens and statistical analysis to determine the repeatability standard deviation for each set. Since the contour method is a destructive measurement technique that requires physically sectioning the specimen (details below), it is impossible to repeatedly measure the same specimen. Thus, a set of specimens was prepared for each configuration and care was taken to obtain specimens with consistent residual stress distributions. The following is a brief description of each configuration.

2.2. GEOMETRY AND MATERIAL

2.2.1. Aluminum T-section

Aluminum T-section specimens were fabricated from bars cut from 82.55 mm (3.25 in) thick 7050-T7451 aluminum plate that had been stress relieved by stretching. The bars had a length of 762 mm (30.0 in), a height of 82.55 mm (3.25 in), and a width of 82.55 mm (3.25 in). The bars were heat treated, including a quench, to induce high residual stress indicative of the T74 temper. The heat treatment used the recipe described in [10] that consists of heating the specimens to 477°C (890°F) for 3 hours, quenching in room temperature water, artificial aging at 121°C (250°F) for 8 hours followed by additional aging at 177 °C (350 °F) for 8 hours. T-sections were then machined from the bars to represent an airframe structural member. Each T-section had a length of 254 mm (10.0 in), a height of

50.8 mm (2.0 in), a width of 82.55 mm (3.25 in), and a leg thicknesses of 6.35 mm (0.25 in), as shown in Figure 1.

2.2.2. Stainless Steel DM Welded Plate

Stainless steel dissimilar metal (DM) weld specimens were fabricated from one long plate made of high-strength 316L stainless steel. The plate had a 25.4 mm (1.0 in) thick by 152.4 mm (6.0 in) wide cross-section and a length of 1.22 m (48.0 in). A slot was machined along the entire length of the plate at the mid-width, and was 9.53 mm (0.375 in) deep and 19.05 mm (0.75 in) wide, with a 70º root angle. The slot and plate cross-section can be seen in Figure 2. Prior to filling the slot with weld material, the plate was constrained by welding it to an additional support plate. The weld joining the plate to the support plate was a continuous 7.94 mm (0.313 in) fillet weld that was applied along both 1.22 m edges of the plate. The slot weld was made using eight passes, each continuous along the entire length of the plate, using an automated welder and 0.89 mm (0.035 in) diameter A52M (ERNiCrFe-7A) wire. Welding was gas tungsten arc welding (GTAW) with 250 A current, 10.5 V voltage, and 101.6 mm/min (4 in/min) travel speed.

Following welding, the DM weld was prepared for measurements. First, the fillet welds were machined away to release the DM weld from the support plate. Second, the ends of the DM weld plate were removed to eliminate the inconsistent weld bead geometry at the start and stop of the weld (139.7 mm (5.5 in) of material was removed from the weld start and 63.5 mm (2.5 in) was removed from the weld stop). The remaining section was 1.02 m (40.0 in) long, and was used for measurements.

2.2.3. Titanium Electron Beam Welded Plate

Titanium alloy electron beam (EB) welded plate specimens were fabricated using one long Ti-6Al-4V plate, with similar geometry to the stainless steel DM welded plate (same cross-section and slot dimensions). The weld process is a typical additive manufacturing process, but service parts would

typically be subjected to thermal stress relief. The groove was filled along the entire length of the plate with 8-passes of 3.18 mm (0.125 in) diameter Ti-6Al-4V wire. After completion of the weld, the plate was sectioned into 101.6 mm (4.0 in) long pieces, as shown in Figure 3.

2.2.4.Stainless Steel Forging

Stainless steel (304L) forging specimens are roughly hemispherical with an outer diameter of 73.7 mm (2.9 in). They include a forged internal cavity with inner diameter of 30.5 mm (1.2 in), and a height of 50.8 mm (2.0 in) (Figure 4). The specimens were produced using a multi-stage forging process. The specimen billets were heated to 980°C (1800°F) for 60 min, die pressed to 75% of their original height in a hydraulic press, cooled to room temperature, heated to 955°C (1750°F) for 60 min, and subjected to a high rate of energy forging operation. Next, the specimens were cooled to room temperature, annealed at 955°C (1750°F) for 30 min, and then water quenched. The final processing steps consisted of reheating the specimens to 845°C (1550°F) for 60 min, a final high rate of energy forging operation, followed by a final water quench.

2.2.5.Nickel Alloy Disk

Nickel alloy (Udimet-720Li) disk specimens had a diameter of 151.20 mm (5.95 in) and a maximum height of 70.41 mm (2.77 in), as shown in Figure 5. The specimens were forged and heat treated, including a quench, to achieve desired mechanical properties. The heat treatment consisted of pre-heating the specimens to 1080°C (1975°F), forging to the nominally finished shape, solution heat treating at 1105°C (2020°F), and oil quenching. The specimens were then stabilized at 760°C (1400°F) for 8 hours, air cooled, aged at 650°C (1200°F) for 24 hours and then air cooled to room temperature. Since the amount of available material was limited, three disks were sectioned in half to give six nominally identical half-disk specimens.

2.3. CONTOUR METHOD

The contour method is a residual stress measurement technique that was established by Prime [11]. A contour method measurement will cut a part along a given measurement plane. Deformation of the cut surfaces will occur as a direct result of residual stress release and redistribution. By measuring the deformed cut surface profiles and applying the negative of the measured profile as a displacement boundary condition in a finite element model of the cut part, the residual stress normal to the cut plane is determined. Detailed experimental steps for the contour method have been provided by Prime and DeWald [12]. The most noteworthy aspect of the contour method is that it provides a two-dimensional spatial map of residual stress at the cut plane.

The contour method measurements for each repeatability study followed nominally the same procedure. For each measurement, the specimen was cut in two using a wire electric discharge machine (EDM) while the specimen was rigidly clamped to the EDM frame. The EDM used 0.254 mm (0.01 in) diameter brass wire and skim cutting settings. Following cutting, the profile of each of the two opposing cut faces was measured with a laser scanning profilometer to determine the surface height normal to the cut plane as a function of in-plane position. Surface height data were taken on a grid of points with spacing between 100 and 200 μm in each direction. The two cut surface profiles were then aligned, averaged on a common grid, and the average was fit to a smooth bivariate Fourier series (informed by the difference between the measured and fitted surface profile). Residual stress on the measurement plane was found by applying the negative of the smoothed surface profile as a displacement boundary condition on the cut face in a linear elastic finite element model of the cut part. Each model used the corresponding set of elastic material properties given in Table 1. The finite element mesh used eight-node, linear interpolation brick elements with node spacing of approximately 1 mm along the cut plane and a bias such that node spacing increased with distance from the cut plane.

2.4. REPEATABILITY EXPERIMENTS

For each of the five specimen types described above, a contour method repeatability experiment was performed. The repeatability studies involved performing a single contour method measurement on a set of similar test specimens. Each measurement provided a 2D map of residual stress. All measurements were performed in a consistent manner to assess measurement repeatability.

For the aluminum T-section specimens, contour method measurements were performed at the mid-length of 10 specimens (127 mm (5 in) from each end, as shown in Figure 1). Six titanium welded specimens were measured at the plate mid-length, as shown in Figure 3. The contour method measurements on the stainless steel forgings were performed at the specimen mid-width (shown in Figure 4) for six specimens. For the six nickel alloy (half) disk specimens, contour method measurements were performed at the specimen mid-width (shown in Figure 5). Stress release from sectioning the disks in half was found using a supplemental stress analysis in conjunction with the strain change recorded before and after sectioning (using strain gages at multiple locations). The total hoop stress, including the effect of sectioning, is reported for the disk specimens.

The stainless steel DM weld repeatability study consisted of measurements at different positions along the length of the plate, rather than making measurements in nominally identical specimens removed from the long plate. This was done to preserve the original residual stress field present in the plate, which is more representative of a highly constrained weld employed at pressurized water reactor (PWR) nuclear power plants. The repeatability experiment consisted of five contour method measurements, where each measurement repeatedly cut the plate in half. Figure 2 show that the first measurement (Cut 1) cut the plate in half; the second (Cut 2A) and third measurements (Cut 2B) cut each of the half plates in half; and the fourth (Cut 3A) and fifth measurements (Cut 3B) cut two of the quarter plates in half. Corrections were made to account for the small changes in residual stress as the

specimen size was reduced by previous contour measurements. The corrections used the data from a preceding measurement, as described in [13].

Following completion of the contour method measurements, the mean and repeatability standard deviation were calculated for each repeatability experiment using standard formulae. This provides a 2D stress map of the mean and a 2D map of the repeatability standard deviation.

3. Results

Residual stress 2D maps of mean and repeatability standard deviation for all configurations are shown in Figure 6 through Figure 15. The median, mean, 75th percentile, 95th percentile, and maximum value of the repeatability standard deviation for all configurations are tabulated in Table 2, where these are computed from the population of all positions on the cross-section.

The mean longitudinal residual stress in the aluminum T-section has compressive stress at the left and right edges of the bottom flange (minimum value of approximately -240 MPa) and at the top of the center flange (minimum value of approximately -70 MPa) with tensile stress at the intersection of the bottom and center flanges (peak value of approximately 100 MPa) (Figure 6a). The measured residual stress is similar between the 10 measurements, as indicated by the relatively low repeatability standard deviation (Figure 6b) and as shown by the line plots (Figure 7). The repeatability standard deviation is low at most points (average of 5 MPa), with localized regions at the edges of the bottom and center flanges where the repeatability standard deviations is larger (95th percentile at 13 MPa).

The mean longitudinal residual stress in the stainless steel DM welded plate has tensile stress in the weld area and heat-affected zone (maximum value of approximately 380 MPa) and near the left and right edges of the plate, where it was welded to the support fixture (maximum value of approximately 400 MPa) (Figure 8a). There is compensating compressive stress toward the top of the

plate at the left and right edges (minimum value of approximately -260 MPa). The stress line plots for each individual measurement and the mean (Figure 9) show that the stress in nominally consistent between specimens, with modest differences at the top and bottom of the plate. These data include corrections for prior measurements, but these were small, having peak magnitudes lower than 10 MPa. (If the corrections had not been made, their effects would have increased observed repeatability standard deviation.) Most points had low repeatability standard deviation (average of 17 MPa), but there are localized regions near the part boundary where the repeatability standard deviation is larger (95^{th} percentile at 36 MPa), as shown in Figure 8b.

The mean longitudinal stress in the titanium EB welded plate has tensile stress in the weld area (maximum value of approximately 350 MPa) and compensating compressive stress in the heat-affected zone (minimum value of approximately -200 MPa) (Figure 10a). The line plots in Figure 11 show that the stress is very consistent between specimens. Most points had a low repeatability standard deviation (average of 8 MPa), with localized regions near the part boundary having higher repeatability standard deviations (95^{th} percentile at 17 MPa), as shown in Figure 10b. In this case, the repeatability standard deviation appears to be more spatially uniform over the cross-section than was found in other cases.

The mean hoop stress in the stainless steel forging has tensile stress adjacent to the internal cavity (maximum value of approximately 340 MPa) and compensating compressive stress near the outer surfaces of the forging (minimum value of approximately -260 MPa) (Figure 12a). Five of the six measurements were nominally consistent, with one being a significant outlier (maximum tensile stress was approximately 100 MPa larger than all the other measurements) as is shown in Figure 13. To further illustrate the outlying measurement, line plots of the stress measured in all six specimens are shown in Figure 14. The repeatability standard deviation reported in Figure 12b, which omits the outlier measurement, has a low repeatability standard deviation (mean at 24 MPa) with localized regions having

higher repeatability standard deviations (95th percentile at 52 MPa). (The repeatability standard deviation including the outlier measurement is larger, with values up to 135 MPa near the forging cavity.)

The mean hoop stress in the nickel disk has tensile stress towards the disk inner diameter at mid-thickness (maximum value of approximately 450 MPa) and compensating compressive stress toward the disk periphery (minimum value of approximately -580 MPa) (Figure 15a). Line plots (Figure 16) show that the measurements are very consistent relative to magnitude of stresses being measured. The repeatability standard deviation distribution is consistent with those from the other configurations, but with more spatial variation over the cross-section. Most points have a modest repeatability standard deviation (average of 25 MPa) and localized regions of high repeatability standard deviation (95th percentile at 52 MPa), particularly near the top and bottom of the disk (Figure 15b).

4. Discussion

The present repeatability data have certain limitations. First, as noted in the introduction, the repeatability standard deviations relate to measurement precision but not accuracy; therefore, they do not address bias and systematic errors that may occur, including errors from elastic bulge [14] or plasticity [15]. Second, the repeatability data are limited by the assumption that specimens within each group are identical and have the same residual stress. Since some of the differences in the measured stress are likely due to part-to-part variability, the reported repeatability standard deviations likely are larger than the true repeatability standard deviation (without part-to-part stress variability). Third, the repeatability standard deviations are derived from a data reduction process that employs a specific form for the surface profile data fit. The choice of fitting function can change the repeatability standard deviation [16] to a small degree (around 5 MPa the aluminum bars shown in [8] and [16]).

The present repeatability experiments provide results consistent with those reported in earlier work [8,9]. In the study using aluminum bars [8], both the measured stress magnitude and the repeatability standard deviation were very similar to the results found in the present aluminum T-section. The stress field in the T-section appears to have the characteristic compressive stress toward the exterior edges and tensile stress toward the center. The repeatability standard deviation was below 10 MPa at most points with maximum values near the part perimeter at 20 MPa for both bar and T-section. Similarly, in a study using a stainless steel plate with a stainless steel slot-filled weld [9], the repeatability standard deviation was below 20 MPa at most points, which is very close to the values found in the stainless steel DM welded plate reported here.

To better understand the distribution of the repeatability standard deviation, histograms were prepared for all samples (Figure 17). Histograms were made for all points, near surface points, within 1 mm of the specimen boundary, and interior points further than 1 mm from the specimen boundary. The histograms show that all configurations exhibit similar trends, where the repeatability standard deviation is largest for points within 1 mm of the specimen boundary and smallest for points that are greater than 1 mm from the boundary. The histograms also suggest that the repeatability standard deviations follow a log-normal distribution. Log-normal probability plots of repeatability standard deviations are shown in Figure 18 for all points, for near surface points within 1 mm of the specimen boundary, and for interior points that are farther than 1 mm from the specimen. Repeatability standard deviations for all configurations is fit well by a log-normal distribution, especially when the near surface and interior points are separated from one another. The 50% probability repeatability standard deviation for near-surface points is about twice that of interior points in all configurations. The 50% probability repeatability standard deviation is nearly equal to the median value shown in Table 2 for all configurations, as expected.

The repeatability standard deviation trend found among the five configurations is consistent. There tends to be relatively stable and low magnitude repeatability standard deviation over most of the specimen interior and localized regions of higher variability along the part perimeter. The magnitude of the repeatability standard deviation increases with elastic modulus of the material, as shown in Figure 19a. To better interpret the results, the mean, median, 75^{th} percentile, and 95^{th} percentile of the repeatability standard deviation for each configuration are shown. The configurations with larger elastic moduli have larger repeatability standard deviations. The median is lower than the mean, which suggests the distribution of repeatability standard deviation is skewed toward larger values. The trends are consistent across cross-sectional shapes and underlying processes (quenching, forging, welding).

To illustrate the correlation between contour method measurement repeatability standard deviation and elastic modulus, the mean and 95^{th} percentile of the repeatability standard deviation are normalized by elastic modulus in Figure 19b. The results show that the normalized mean repeatability standard deviation is relatively consistent across all specimens, ranging from 70×10^{-6} MPa/MPa to 125×10^{-6} MPa/MPa, with an average value of approximately 100×10^{-6} MPa/MPa. The 95^{th} percentile of the normalized repeatability standard deviation was also relatively consistent, but covers a significantly larger range from 150×10^{-6} MPa/MPa to 275×10^{-6} MPa/MPa, with an average value of 220×10^{-6} MPa/MPa. Data from the two earlier contour method repeatability studies [8,9] also fit the same trend.

Since the repeatability standard deviation normalized by elastic modulus appears to be relatively constant, the *point-wise average* precision of the contour method, which is quantified by the repeatability standard deviation for a generic part can be estimated as $100 \times 10^{-6}E$, where E is the elastic modulus. This estimate assumes best case precision and is appropriate for points in the cross-section interior.

5. Summary/Conclusions

Contour method repeatability was determined in five configurations: an aluminum T-section, a stainless steel plate with a dissimilar metal slot-filled weld, a stainless steel forging, a titanium plate with an electron beam slot-filled weld, and a nickel disk forging. For each configuration, 5 to 10 contour method measurements were assessed to determine the spatial distribution of repeatability standard deviation. The results show consistent levels of repeatability over most of the specimen interior and localized regions of higher variability (typically along the part perimeter). The mean repeatability standard deviation scales with elastic modulus, E, and was equal to approximately $100 \times 10^{-6}E$. The mean repeatability standard deviation ranged from 5 MPa for the aluminum T-section to 25 MPa for the nickel disk forging, which represent the minimum and maximum values among the configurations. Similarly, the value of the 95th percentile repeatability standard deviation ranged from 13 MPa for the aluminum T-section to 52 MPa for the stainless steel forging.

6. Acknowledgements

The authors acknowledge, with gratitude, the U.S. Air Force for providing financial support for this work (contract FA8650- 14-C-5026). We would also like to acknowledge Steve McCracken from the Electric Power Research Institute for suppling and fabricating the stainless steel plate with a dissimilar metal slot-filled weld, Thomas Reynolds from Sandia National Laboratory for providing the stainless steel forgings, and Brian Streich from Honeywell for providing the nickel disk forgings.

References

[1] E11 Committee, “Practice for Use of the Terms Precision and Bias in ASTM Test Methods,” ASTM International, West Conshohocken, PA, Oct. 2010.

[2] S. Lestari, “Residual Stress Measurements of Unblasted and Sandblasted Mild Steel Specimens Using X-Ray Diffraction, Strain-Gage Hole Drilling, and Electronic Speckle Pattern Interferometry (ESPI) Hole Drilling Methods,” University of New Orleans, 2004.

[3] M. D. Olson, J. S. Robinson, R. C. Wimpory, and M. R. Hill, "Characterisation of residual stresses in heat treated, high strength aluminium alloy extrusions," *Mater. Sci. Technol.*, vol. 32, no. 14, pp. 1427–1438, 2016.

[4] M. E. Fitzpatrick and A. Lodini, Analysis of Residual Stress by Diffraction using Neutron and Synchrotron Radiation. CRC Press, 2003.

[5] M. B. Prime, T. Gnäupel-Herold, J. A. Baumann, R. J. Lederich, D. M. Bowden, and R. J. Sebring, "Residual stress measurements in a thick, dissimilar aluminum alloy friction stir weld," *Acta Mater.*, vol. 54, no. 15, pp. 4013–4021, Sep. 2006.

[6] D. Upshaw, M. Steinzig, and J. Rasty, "Influence of Drilling Parameters on the Accuracy of Hole-drilling Residual Stress Measurements," in *Engineering Applications of Residual Stress*, Volume 8, Springer New York, 2011, pp. 95–109.

[7] M. Steinzig and T. Takahashi, "Residual Stress Measurement Using The Hole Drilling Method And Laser Speckle Interferometry Part IV: Measurement Accuracy," *Exp. Tech.*, vol. 27, no. 6, pp. 59–63, Nov. 2003.

[8] M. R. Hill and M. D. Olson, "Repeatability of the Contour Method for Residual Stress Measurement," *Exp. Mech.*, vol. 54, no. 7, pp. 1269–1277, Sep. 2014.

[9] M. D. Olson, M. R. Hill, E. Willis, A. G. Peterson, V. I. Patel, and O. Muránsky, "Assessment of Weld Residual Stress Measurement Precision: Mock-Up Design and Results for the Contour Method," *Journal of Nuclear Engineering and Radiation Science*, 2015.

[10] SAE Aerospace, "Aerospace Material Specification 4342: Aluminum Alloy Extrusions: Solution Heat Treated, Stress Relieved, Straightened, and Overaged," 2006.

[11] M. B. Prime, "Cross-Sectional Mapping of Residual Stresses by Measuring the Surface Contour After a Cut," *J. Eng. Mater. Technol.*, vol. 123, no. 2, pp. 162–168, Apr. 2001.

[12] M. B. Prime and A. T. DeWald, "The Contour Method," in Practical Residual Stress Measurement Methods, Ch 5, G. S. Schajer, Ed. West Sussex, UK: John Wiley & Sons, Ltd, 2013, pp. 109–138.

[13] W. Wong and M. R. Hill, "Superposition and Destructive Residual Stress Measurements," *Exp. Mech.*, vol. 53, no. 3, pp. 339–344, Mar. 2013.

[14] M. B. Prime and A. L. Kastengren, "The Contour Method Cutting Assumption: Error Minimization and Correction," in *Proceedings of the SEM Annual Conference & Exposition on Experimental and Applied Mechanics*, 2010.

[15] Y. L. Sun, M. J. Roy, A. N. Vasileiou, M. C. Smith, J. A. Francis, and F. Hosseinzadeh, "Evaluation of Errors Associated with Cutting-Induced Plasticity in Residual Stress Measurements Using the Contour Method," *Exp. Mech.*, pp. 1–16, Feb. 2017.

[16] M. D. Olson, "Importance of Surface Fitting Parameters for Repeatability of the Contour Method," presented at the Residual Stress Summit 2013, Idaho Falls, ID, USA, 10-Oct-2013.

Tables

Specimen	Elastic Modulus (GPa)	Poisson's Ratio	Yield Strength (MPa)
Aluminum T-section (7085-T74)	71	0.33	460
Titanium EB welded plate (Ti-6Al-4V)	110	0.31	960
Nickel disk (Udimet-720Li)	200	0.31	300-500
Stainless steel forging (304L)	200	0.249	470
Stainless steel DM welded plate (316L plate)	203	0.3	440
Stainless steel DM welded plate (A52 weld)	211	0.289	345-482

Table 1: Material properties for each of the specimens used in the repeatability studies

Specimen	Median (MPa)	Mean (MPa)	75th percentile (MPa)	95th percentile (MPa)	Max (MPa)
Aluminum T-section (7085-T74)	3.7	5.1	6.2	12.6	36.7
Titanium EB welded plate (Ti-6Al-4V)	5.9	7.7	8.3	17.3	130.2
Nickel disk (Udimet-720Li)	21.5	24.9	29.7	51.7	290.9
Stainless steel forging (304L)	20.3	23.8	27.6	52.3	141.3
Stainless steel DM welded plate	14.9	17.3	21.6	36.3	146.5

Table 2: Repeatability standard deviation statistical values

Figures

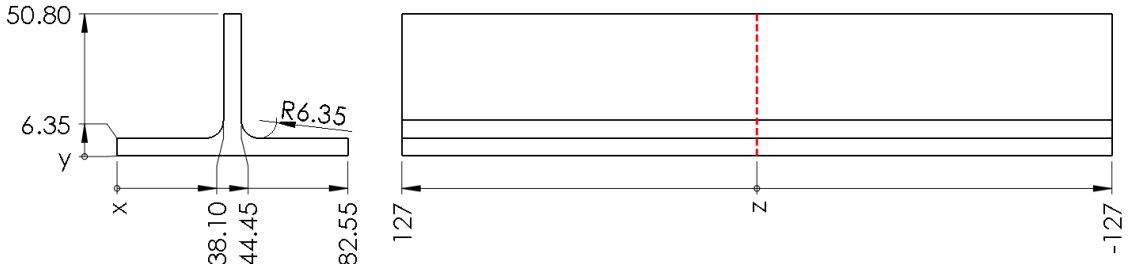

Figure 1: Aluminum T-section dimensions and measurement location (dimensions in mm)

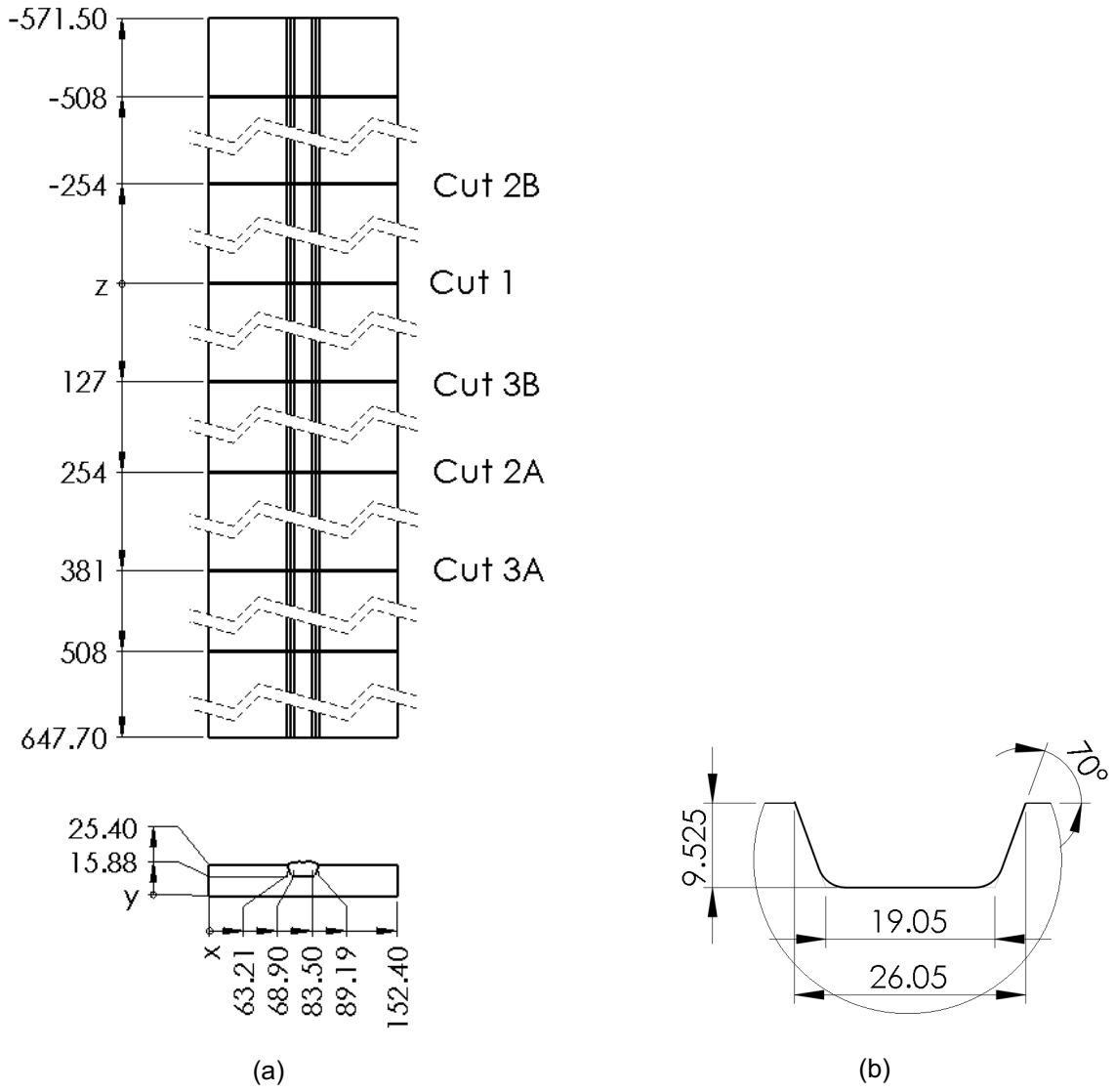

Figure 2: Stainless steel dissimilar metal welded plate (a) dimensions and measurement locations and (b) slot details (dimensions in mm)

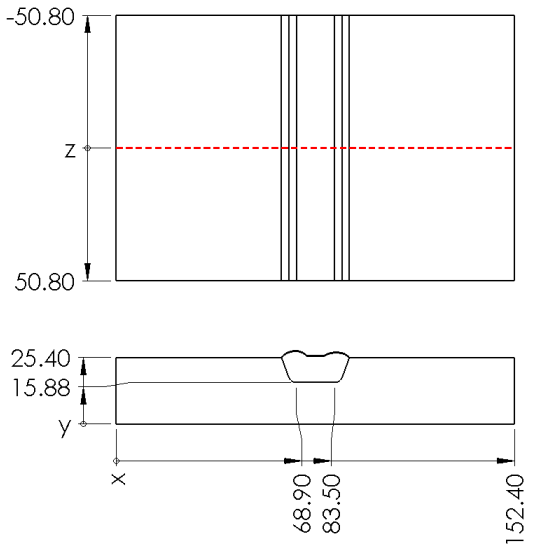

Figure 3: Titanium electron beam welded plate dimensions and measurement location (dimensions in mm)

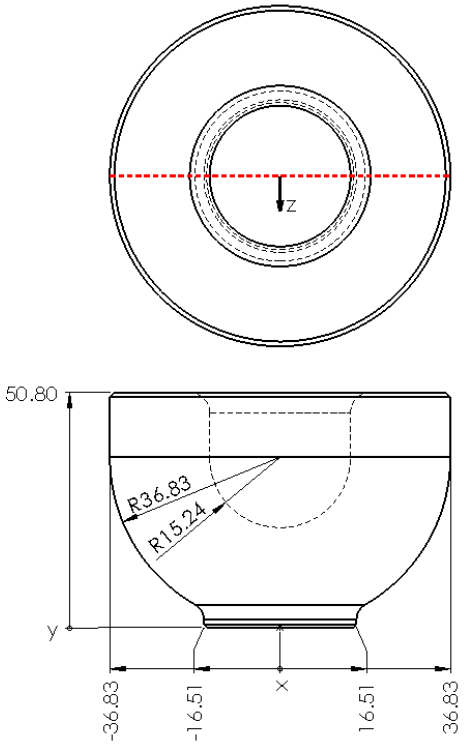

Figure 4: Stainless steel forging dimensions and measurement location (dimensions in mm)

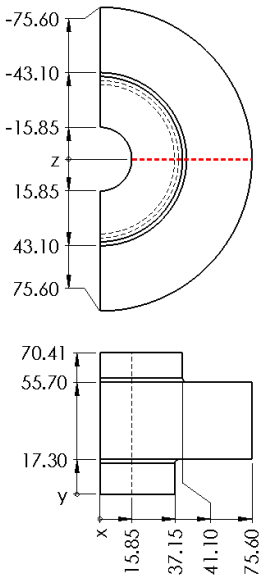

Figure 5: Nickel disk dimensions and measurement location (dimensions in mm)

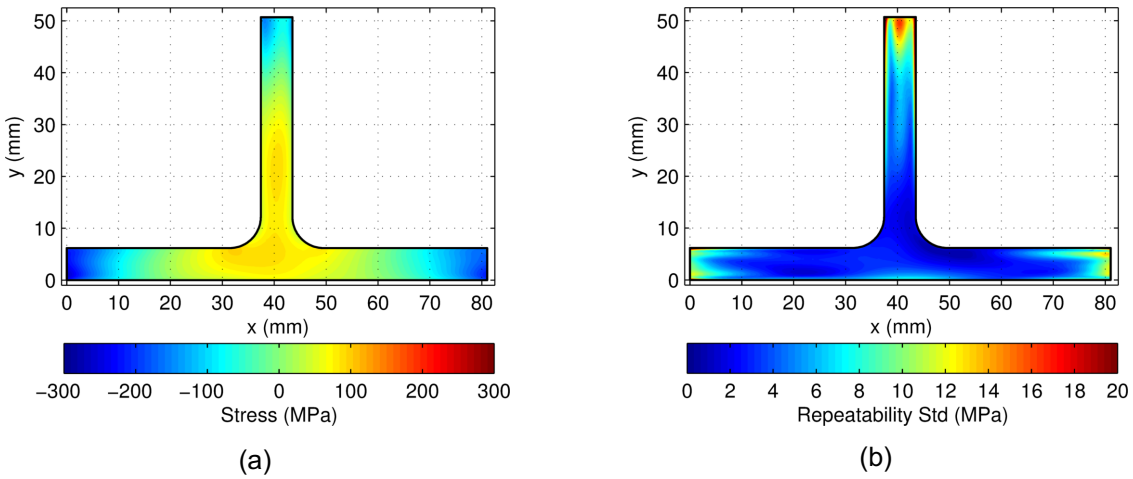

Figure 6: (a) Mean and (b) repeatability standard deviation for the aluminum T-section specimens

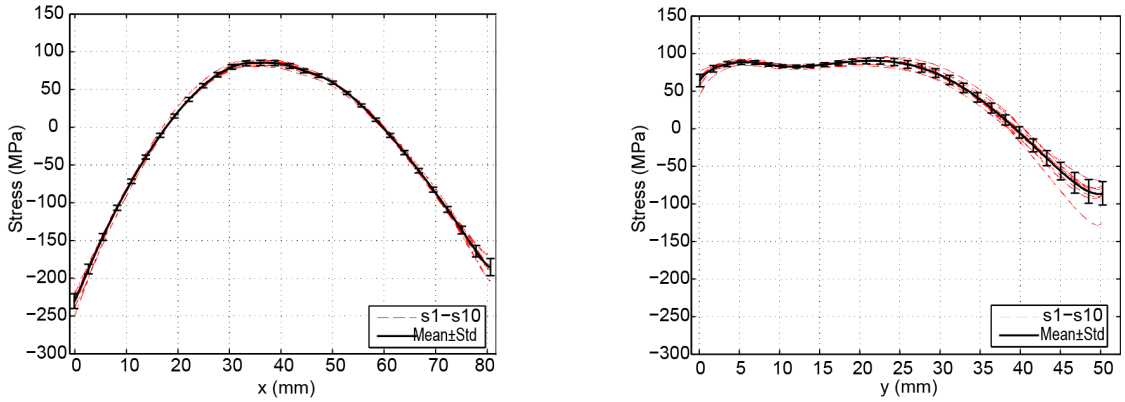

Figure 7: Line plots of individual measurements (dashed red) and the mean and repeatability standard deviation (solid black) for the aluminum T-section samples along the (a) x-direction at y = 3.18 mm and (b) along the y-direction at x = 40.52 mm

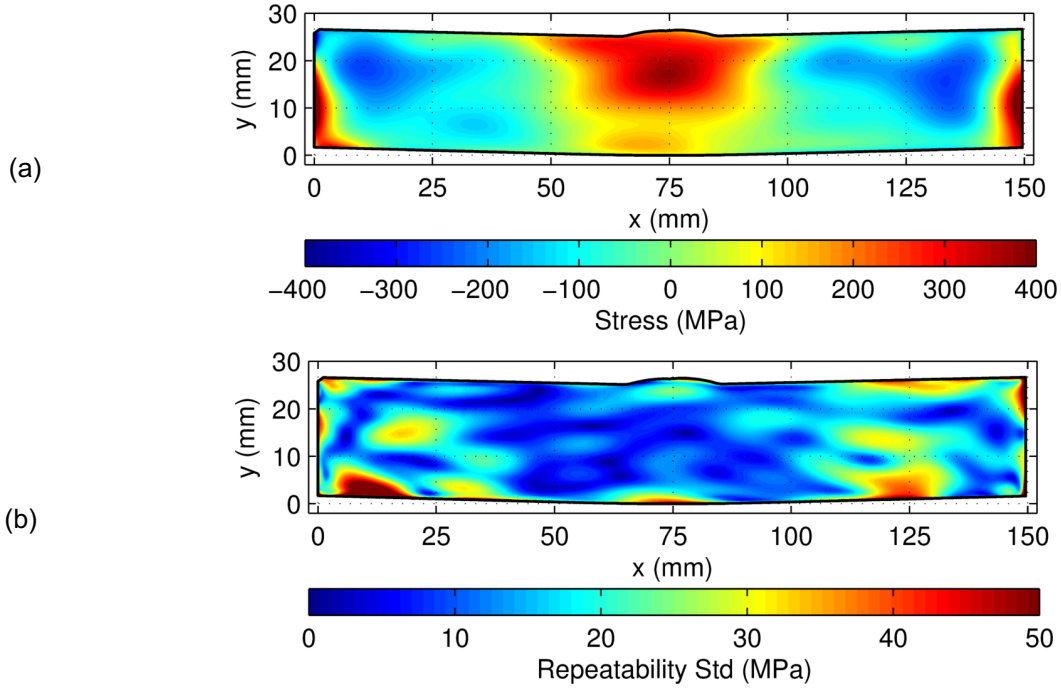

Figure 8: (a) Mean and (b) repeatability standard deviation for the stainless steel DM welded specimens

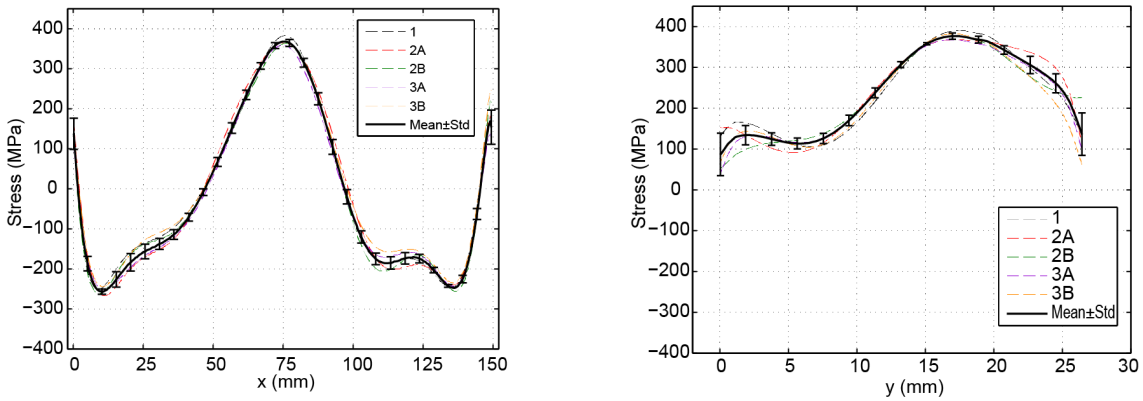

(a) (b)

Figure 9 Line plots of individual measurements (dashed) and the mean and repeatability standard deviation (solid black) for the stainless steel DM welded samples along the (a) x-direction at y = 19.05 mm (weld root) and (b) along the y-direction at x = 76.2 mm (plate mid-width).

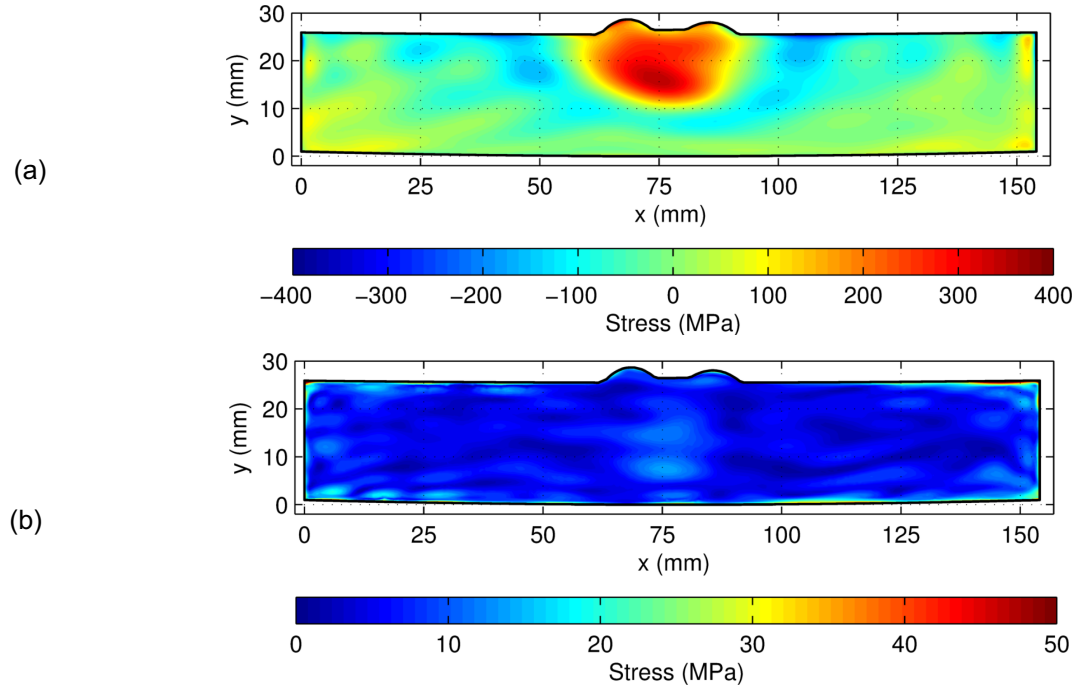

Figure 10: (a) Mean and (b) repeatability standard deviation for the titanium EB welded plate specimens

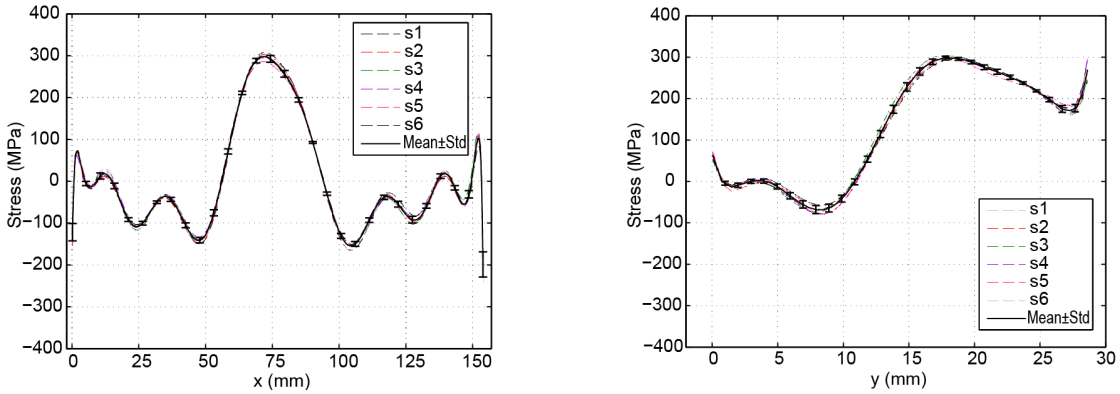

Figure 11: Line plots of individual measurements (dashed) and the mean and repeatability standard deviation (solid black) for the titanium EB welded plate samples along the (a) x-direction at y = 20.32 mm (weld root) and (b) along the y-direction at x = 68.15 mm (center of weld bead)

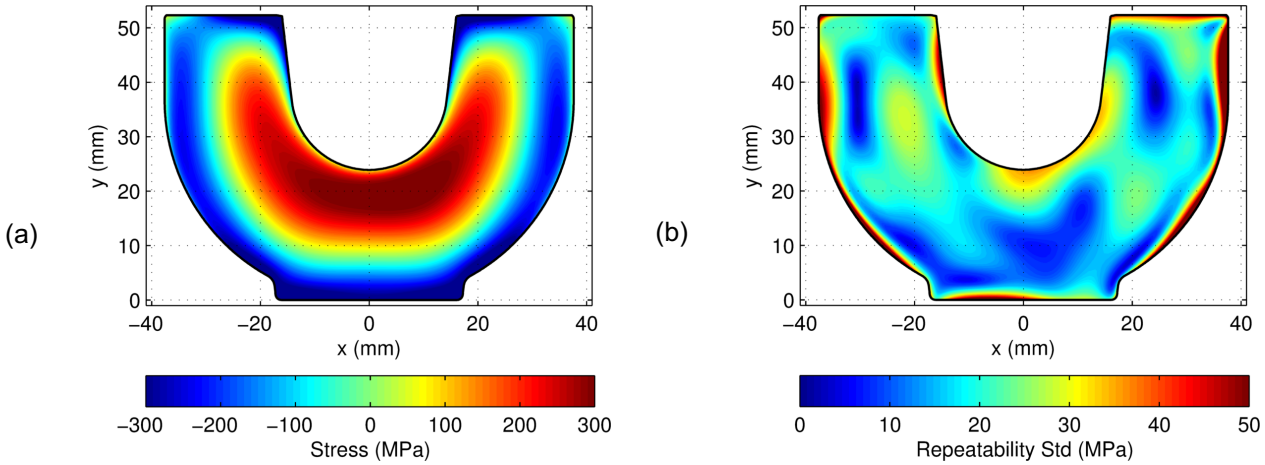

Figure 12: (a) Mean and (b) repeatability standard deviation for the stainless steel forging specimens

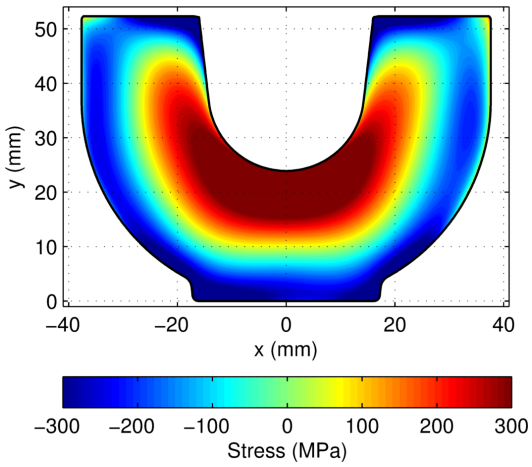

Figure 13: Outling stainless steel forging measurements (S2)

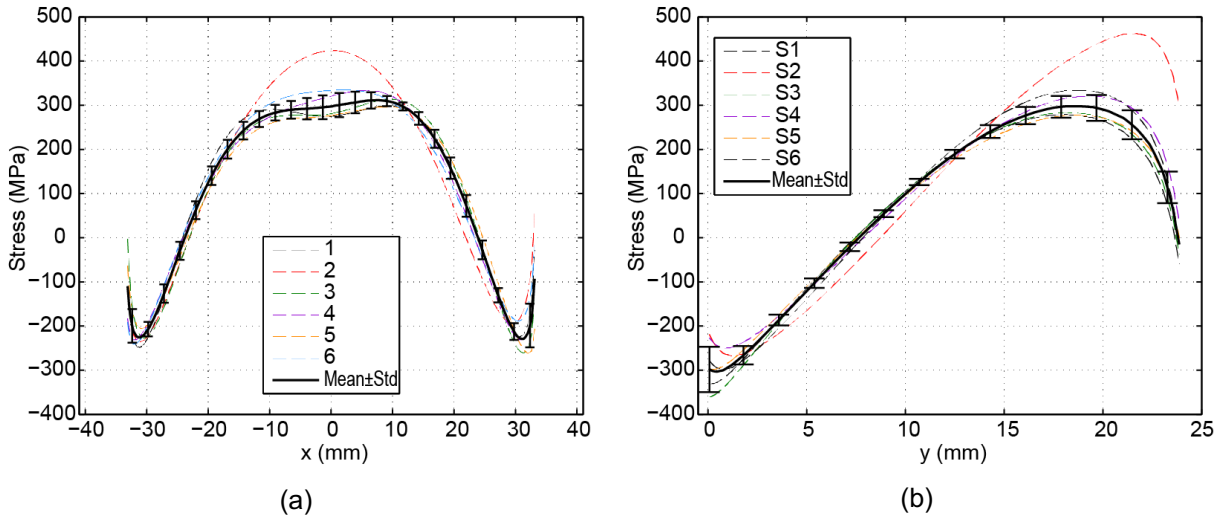

Figure 14: Line plots of individual measurements (dashed) and the mean and repeatability standard deviation (solid black) for the stainless steel forging samples along the (a) x-direction at y = 19.05 mm and (b) along the y-direction at x = 0

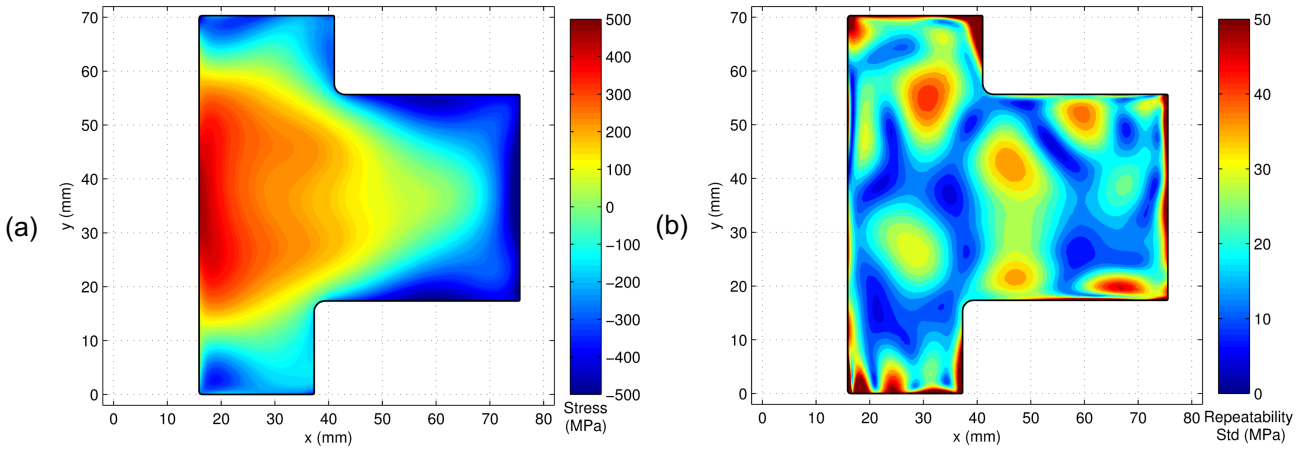

Figure 15: (a) Mean and (b) repeatability standard deviation for the nickel disk specimens

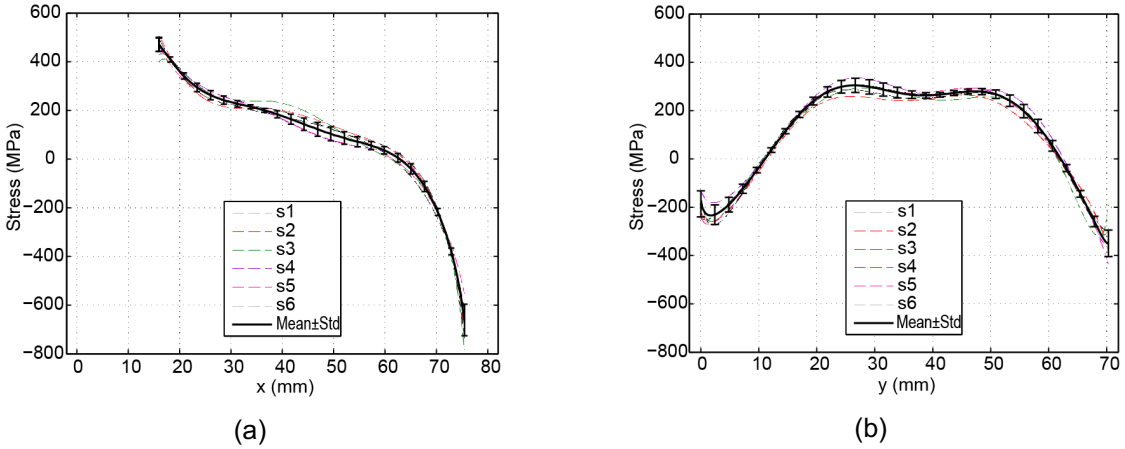

Figure 16: Line plots of individual measurements (dashed) and the mean and repeatability standard deviation (solid black) for the nickel disk samples along the (a) x-direction at y = 35.15 mm (mid-height) and (b) along the y-direction at x = 25.4 mm

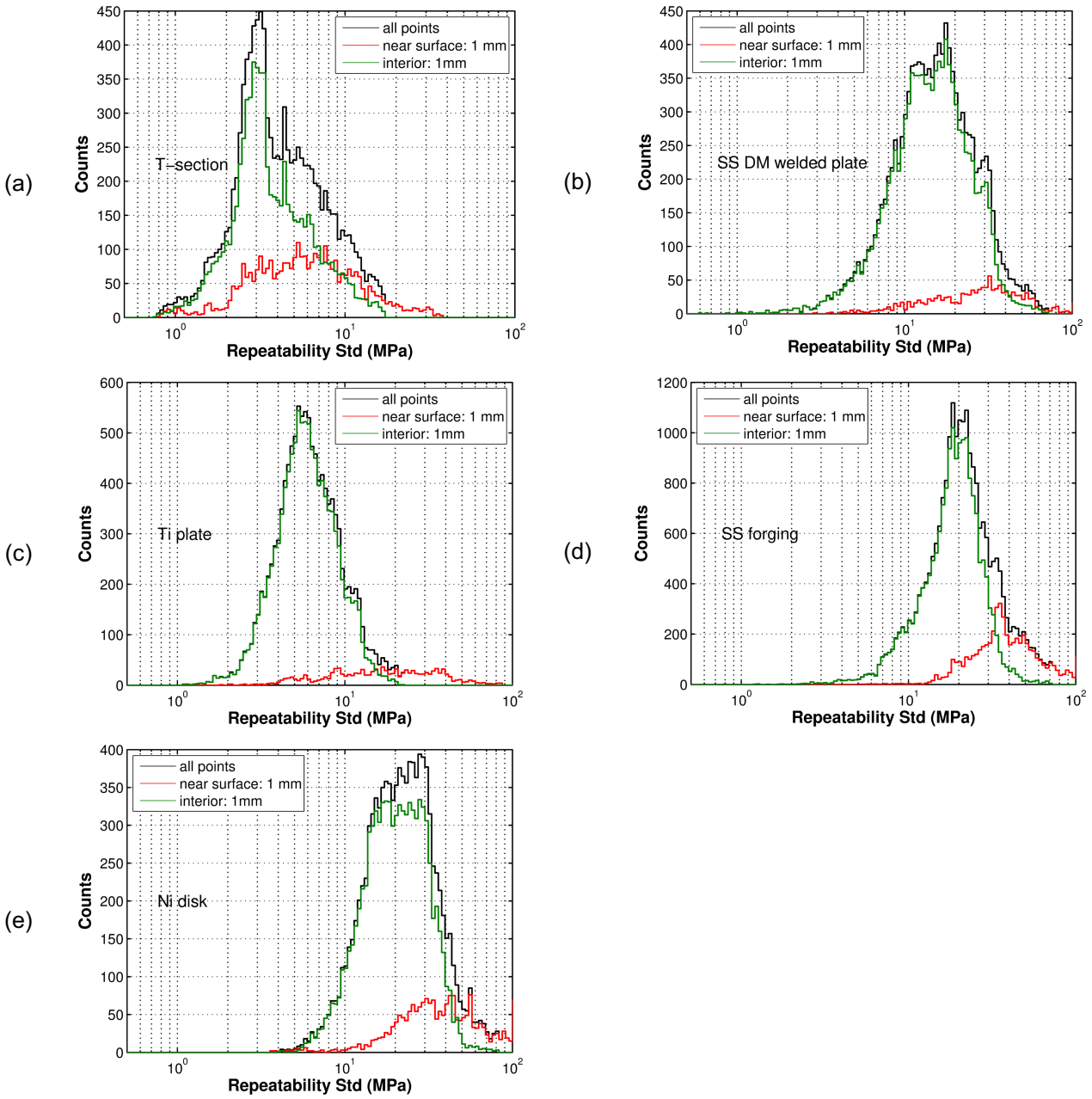

Figure 17: Histogram of the points with a given repeatability standard deviation for the (a) aluminum T-section specimen, (b) the stainless steel DM welded specimen, (c) titanium EB welded plate specimen, (d) the stainless steel forging specimen, and (e) the nickel disk specimen

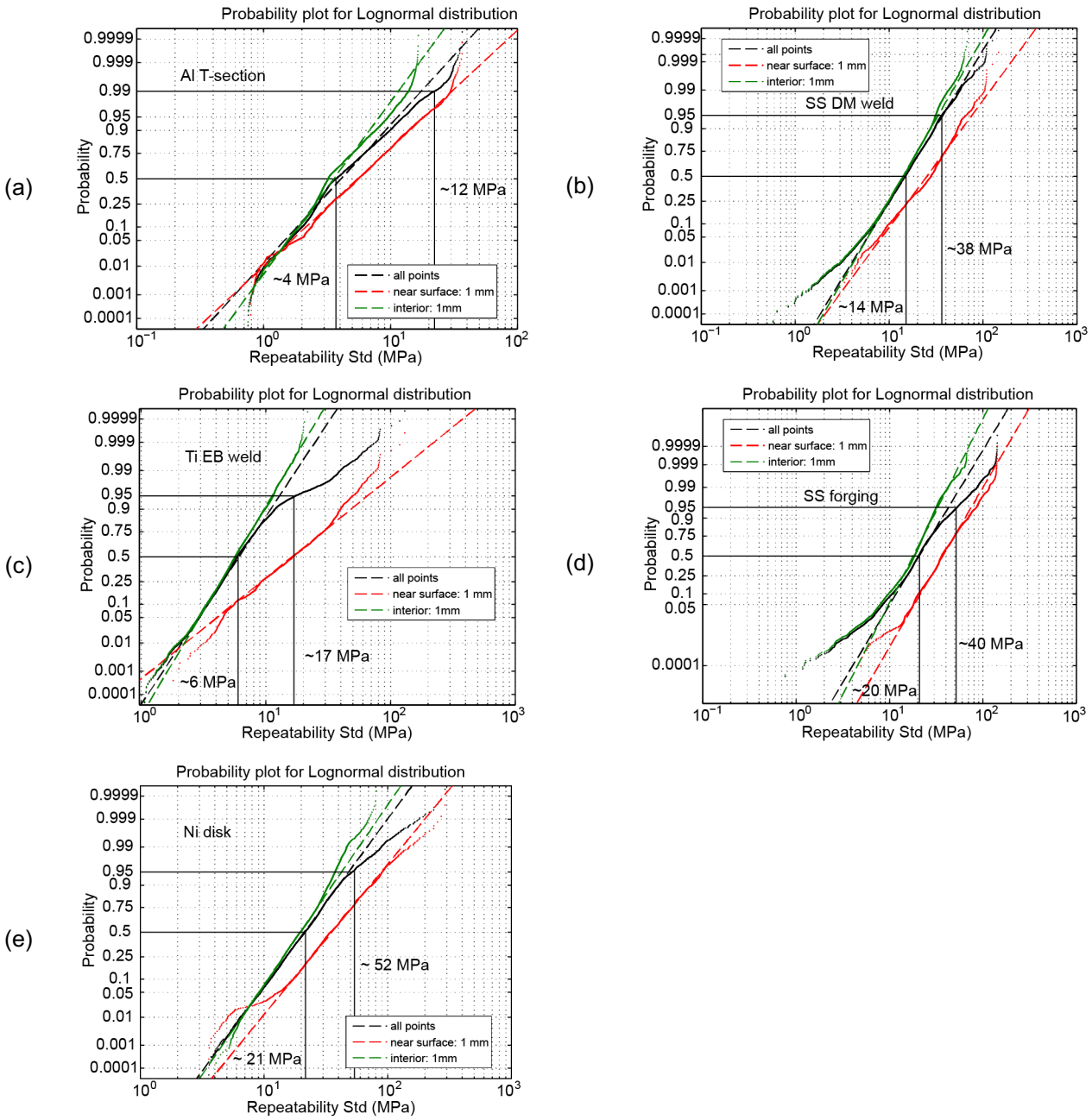

Figure 18: Probablity of a fitted log-normal distribution for the (a) aluminum T-section specimen, (b) the stainless steel DM welded specimen, (c) titanium EB welded plate specimen, (d) the stainless steel forging specimen, and (e) the nickel disk specimen

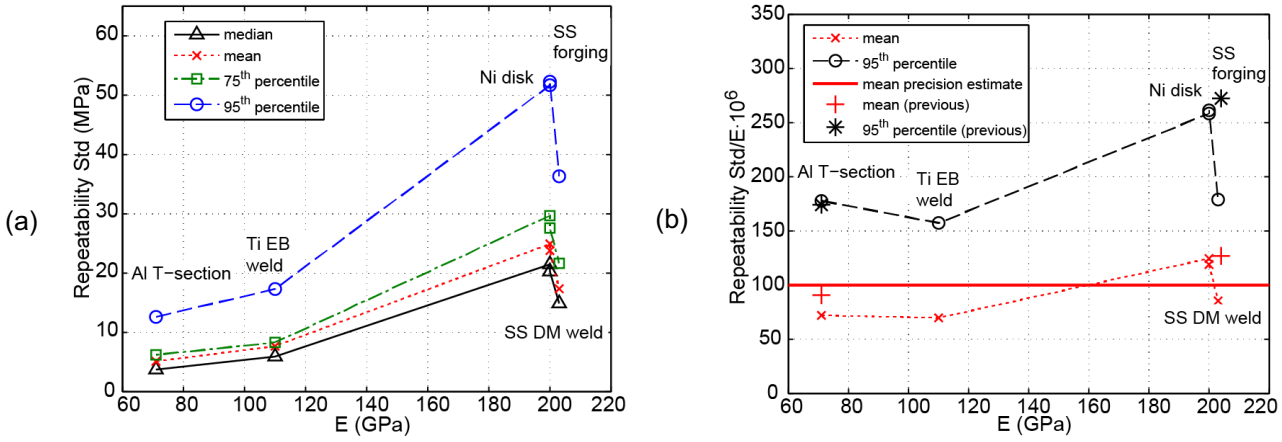

Figure 19: Repeatability standard deviation (a) statistics and (b) statistics normalized by elastic modulus. Previous data in (b) is from a quenched aluminum bar (E = 71 GPa) [8] and a stainless steel plate with a stainless steel slot-filled weld (E = 203 GPa) [9]